

GREAT DESIGNS IN **STEEL**

PROCESS CONSIDERATIONS FOR NIOBIUM IN A TRIP-ASSISTED DP STEEL

Matt Enloe & Fabio D'Aiuto, CBMM NA & CBMM Europe

Hardy Mohrbacher, NiobelCon bvba

OUTLINE

- Background & Motivation
 - Formability Challenges in AHSS
 - Microalloy Effects in AHSS
 - DH Steel Development
- Materials & Methods
 - Alloy Design
 - Process Design
 - Metallurgical Analyses
- Results & Discussion
 - Microstructural Evolution
 - Evolution of Niobium Precipitation
 - Mechanical Performance
- Conclusions



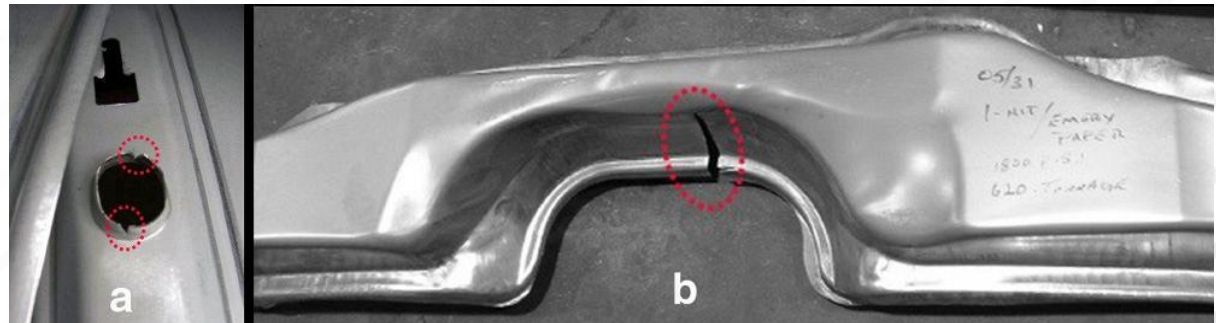
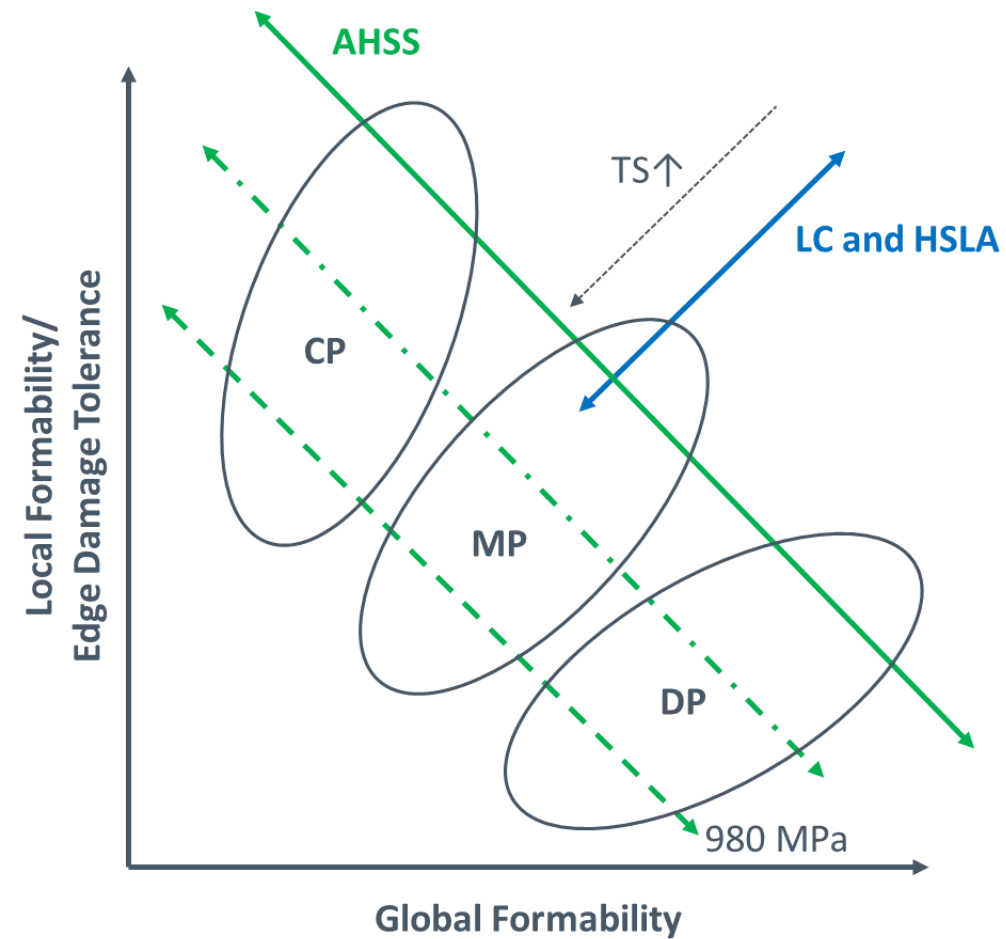
BACKGROUND & MOTIVATION

FORMABILITY CHALLENGES IN AHSS

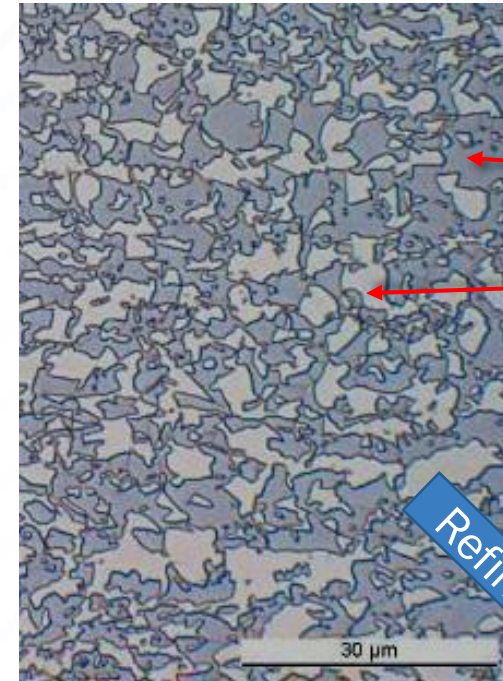
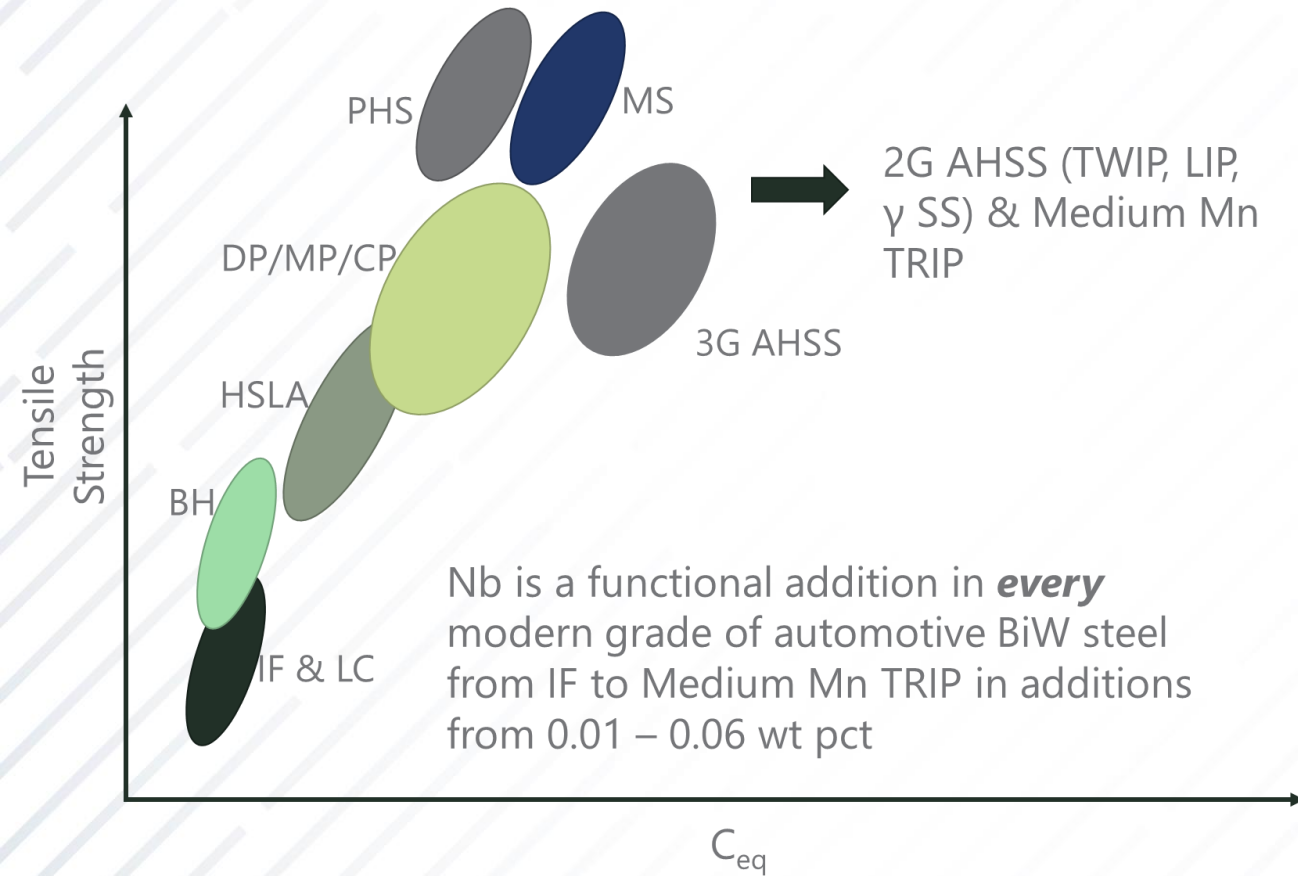
Formability Balance Remains a Challenge in Multiphase Steels

For Conventional Ferritic Steels, Global and Local Formability are Positively Correlated (Shown in Blue)

Global and Local Formability are Negatively Correlated for Multiphase AHSS (Shown in Green)



MICROALLOY EFFECTS IN AHSS



Refinement



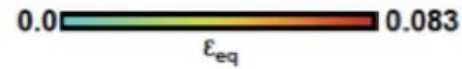
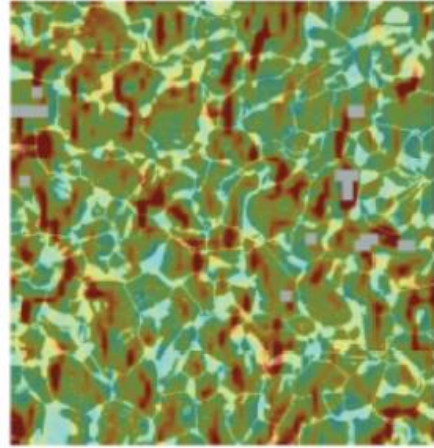
The Effect of Nb: Structural Refinement and Ferrite Strengthening in Multi-phase Steels Improves Formability Balance. Microstructural uniformity and cleanliness remain similarly important to prevention of local fracture.

MICROALLOY EFFECTS IN AHSS

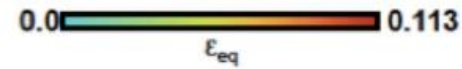
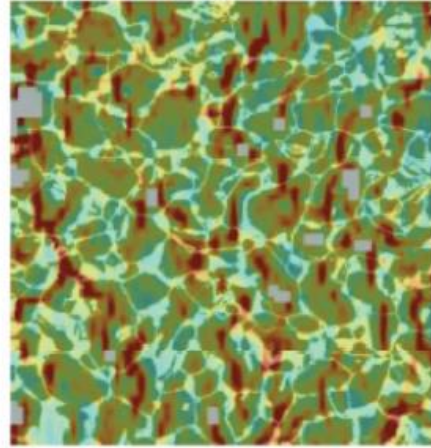
- Strain Distributions more homogeneous in refined structure.



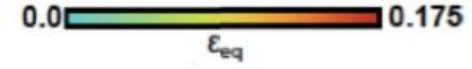
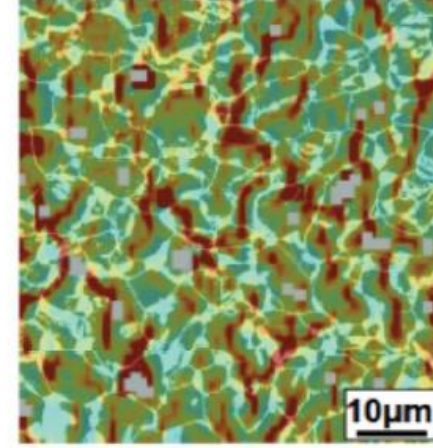
(a) $e = 2.8\%$



(b) $e = 6.5\%$



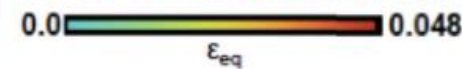
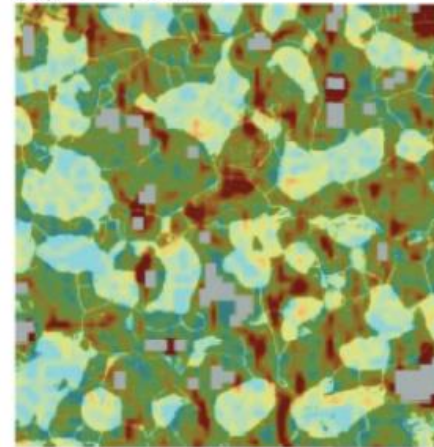
(c) $e = 10.0\%$



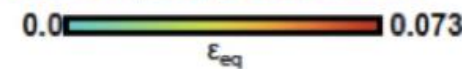
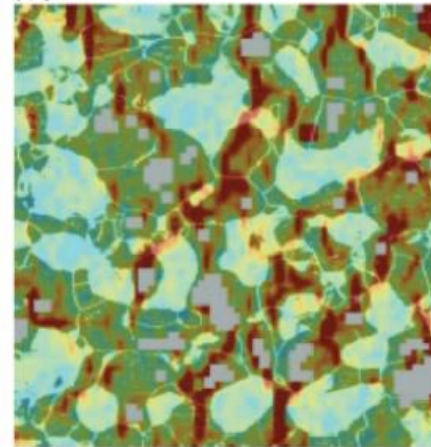
- Strain more localized at F/M interfaces in coarse structure.



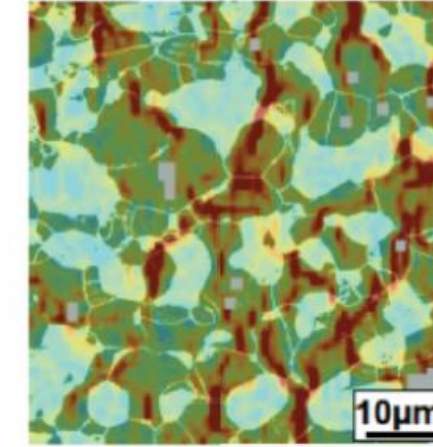
(d) $e = 1.1\%$



(e) $e = 3.7\%$

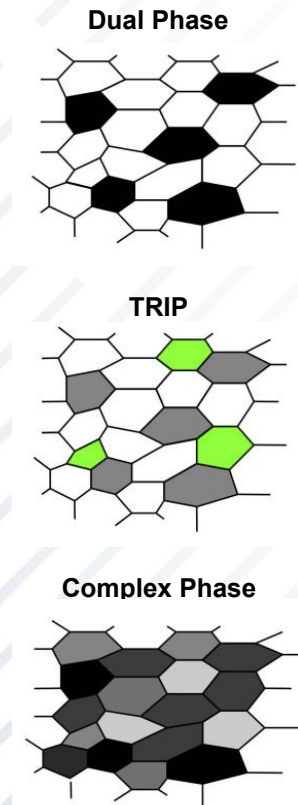


(f) $e = 6.4\%$

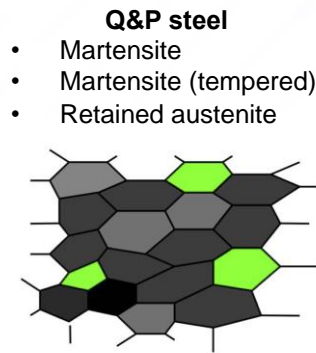
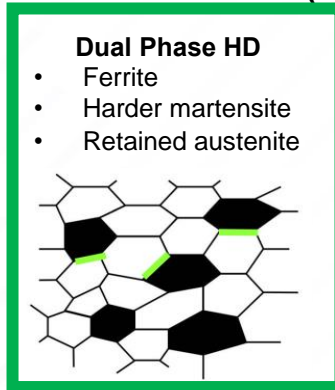


DEVELOPMENT OF HD DP STEELS

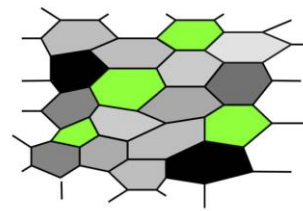
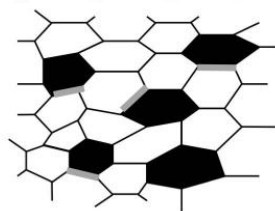
1st generation AHSS
(TS: 450 – 980 MPa)



3rd generation AHSS
(TS: 780 – 1180 MPa)



Microstructural refinement



“High Ductility” (HD) DP steel variants provide increased drawability aided by a small share of austenite retained in the microstructure

This study investigates the microstructural evolution and progress of niobium precipitation during industrial processing of high-ductility DP 980

Stahlgüte / Steel Grade	Streckgrenze / Yield Strength $R_{p0,2}$ MPa	Zugfestigkeit / Tensile Strength R_m MPa	Bruchdehnung / Elongation			n		BH ₂ MPa
			Type 1 $A_{50\text{ mm}}$ %	Type 2 $A_{80\text{ mm}}$ %	Type 3 $A_{50\text{ mm}}$ %	n_{4-6}	$n_{10-20/Ag}$	
CR440Y780T-DH	440 – 550	780 – 900	≥ 19	≥ 18	≥ 19	≥ 0,18	≥ 0,13	≥ 30
CR700Y980T-DH	700 – 850	980 – 1180	≥ 14	≥ 13	≥ 14	-	-	≥ 30

MATERIALS & METHODS

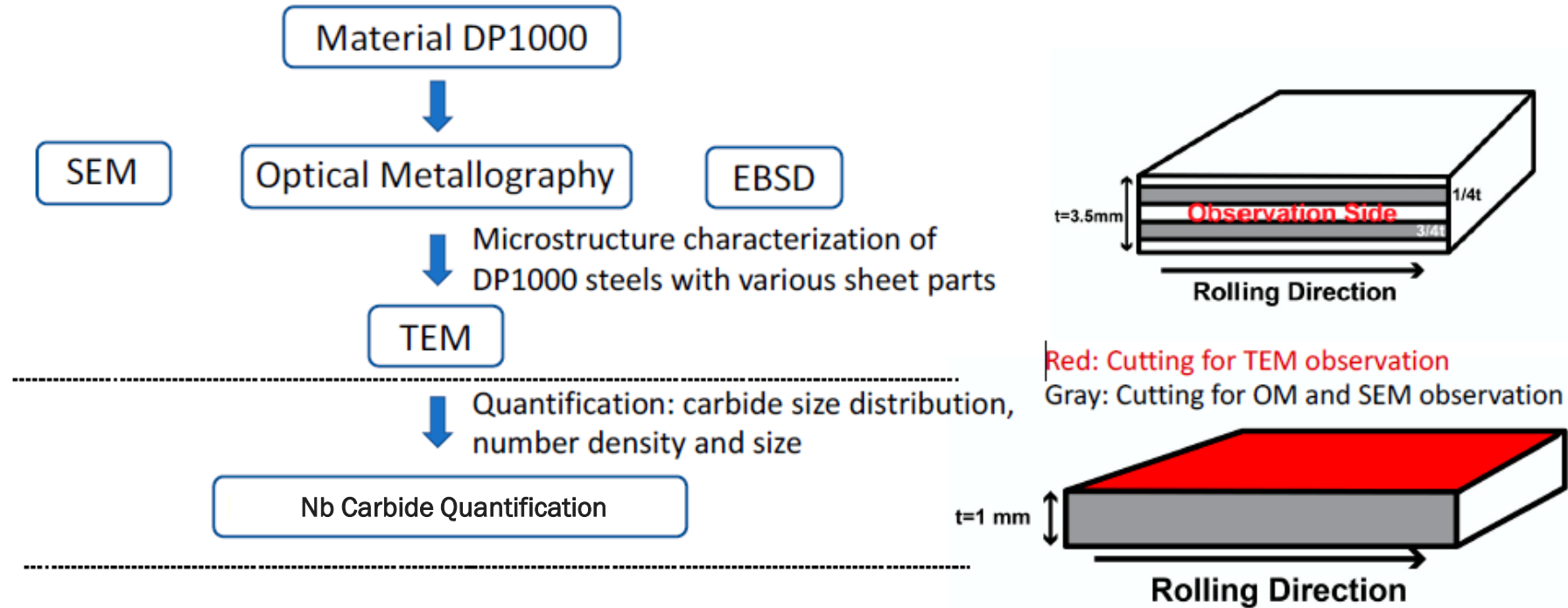
STEEL PRODUCTION PARAMETERS

- C, Mn, and Si increased relative to DP for austenite retention
- Nb included for structural refinement and ferrite strengthening.
- Not TMCP-Rolled
- Batch anneal included following hot rolling to soften for CR (70%) and to spheroidize cementite
- PMT of 850 °C prior to galvanizing

Alloy (Mass%)	C	Mn	Si	Cr	Nb	Ti	B
DP980 HD:	≈0.2	2.2–2.6	0.5–1.0	<0.7	0.03	<0.02	<0.003
Processing Stage	Slab Soaking	Finish Rolling	Coiling		Batch Annealing	Continuous Annealing	
Temperature:	1240 °C	>900 °C	≈600 °C		580 °C/10 h	850 °C	

CHARACTERIZATION

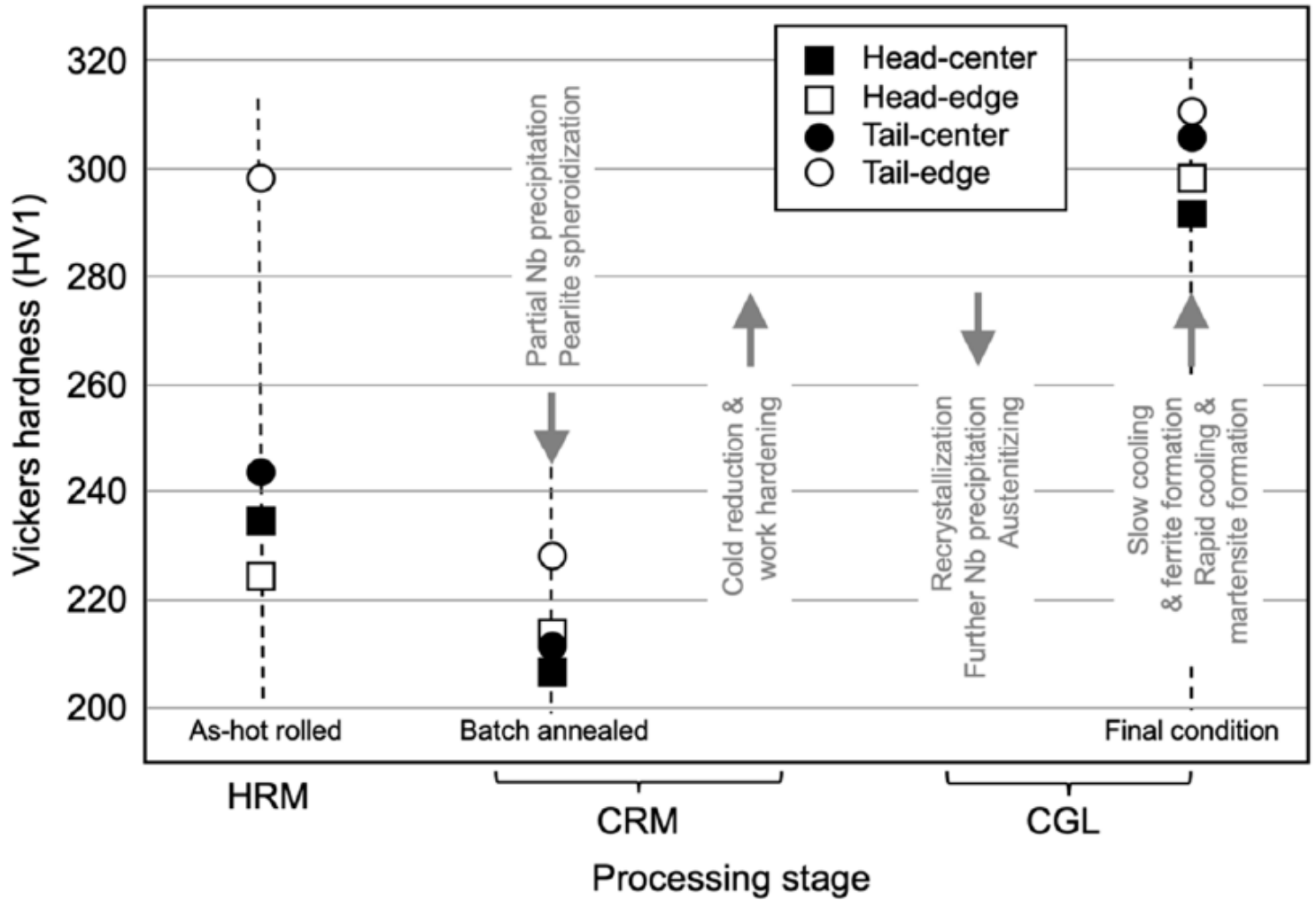
Samples extracted from head and tail, center and edge of hot band, batch annealed, and finished galvanized product.



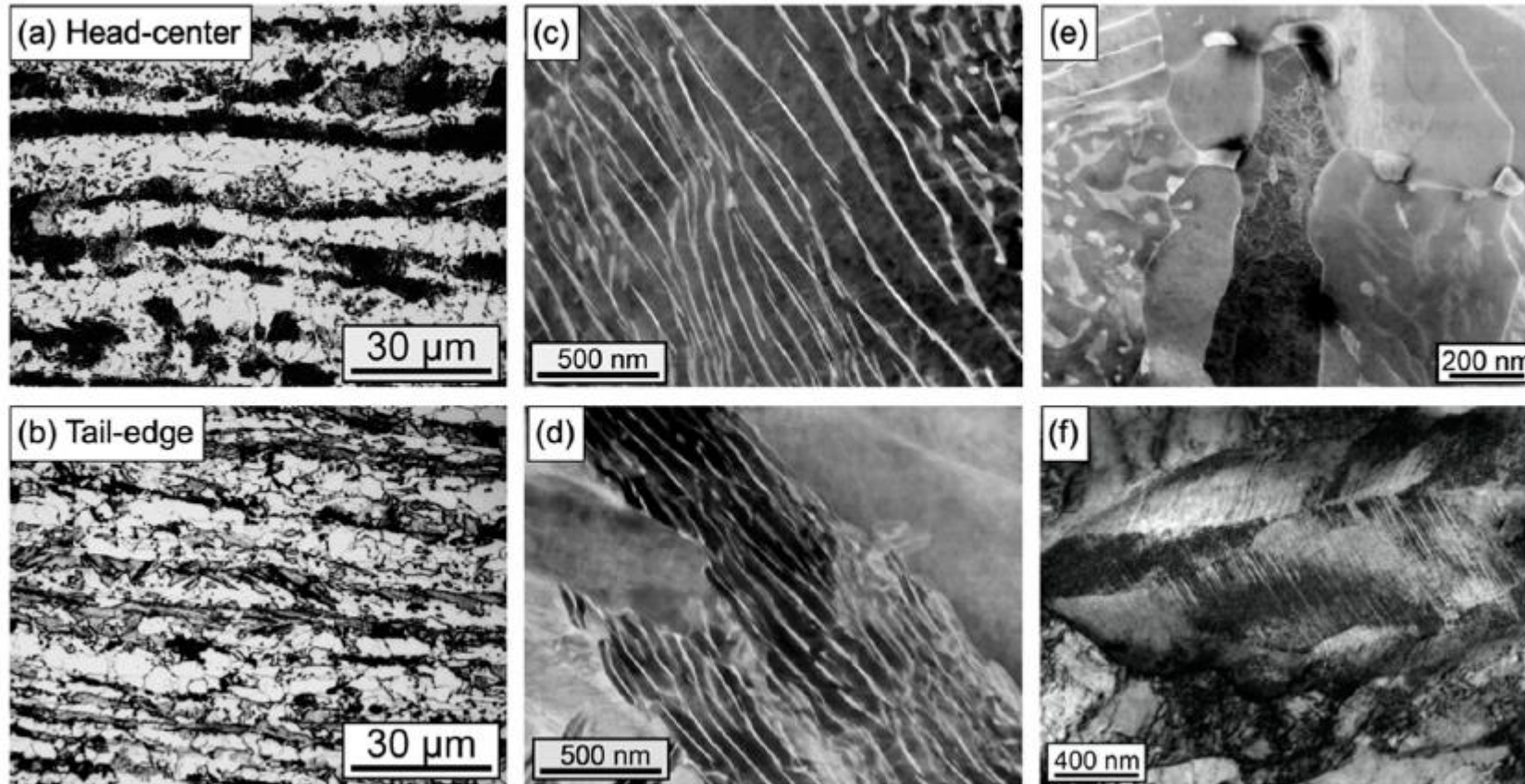
Mechanical evaluations were also conducted to obtain Vickers hardnesses and uniaxial tensile properties.

RESULTS & DISCUSSION

HARDNESS EVOLUTION

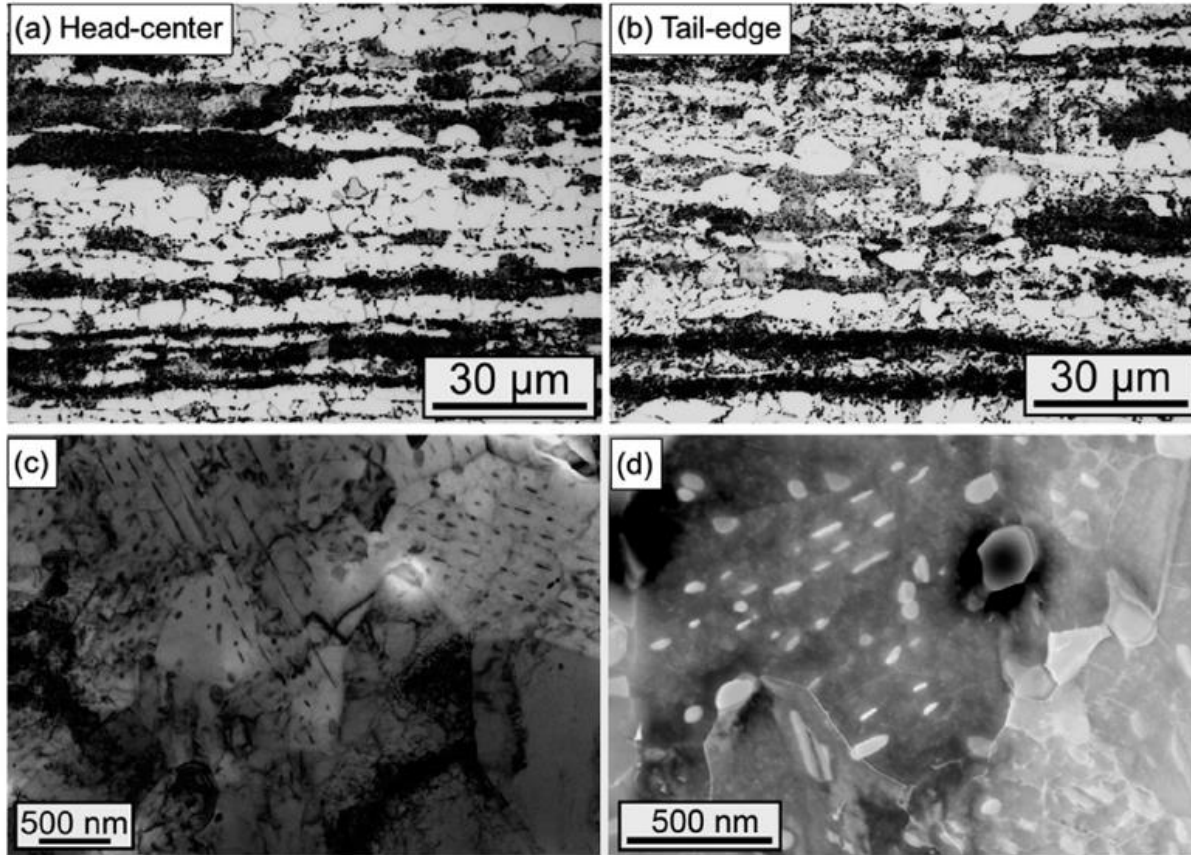


HOT ROLLED MICROSTRUCTURE



Microstructure in as hot rolled condition: (a,b) light optical microscopy; (c,d) TEM (Transmission electron microscope) details of lamellar pearlite; (e,f) TEM details of martensitic phases.

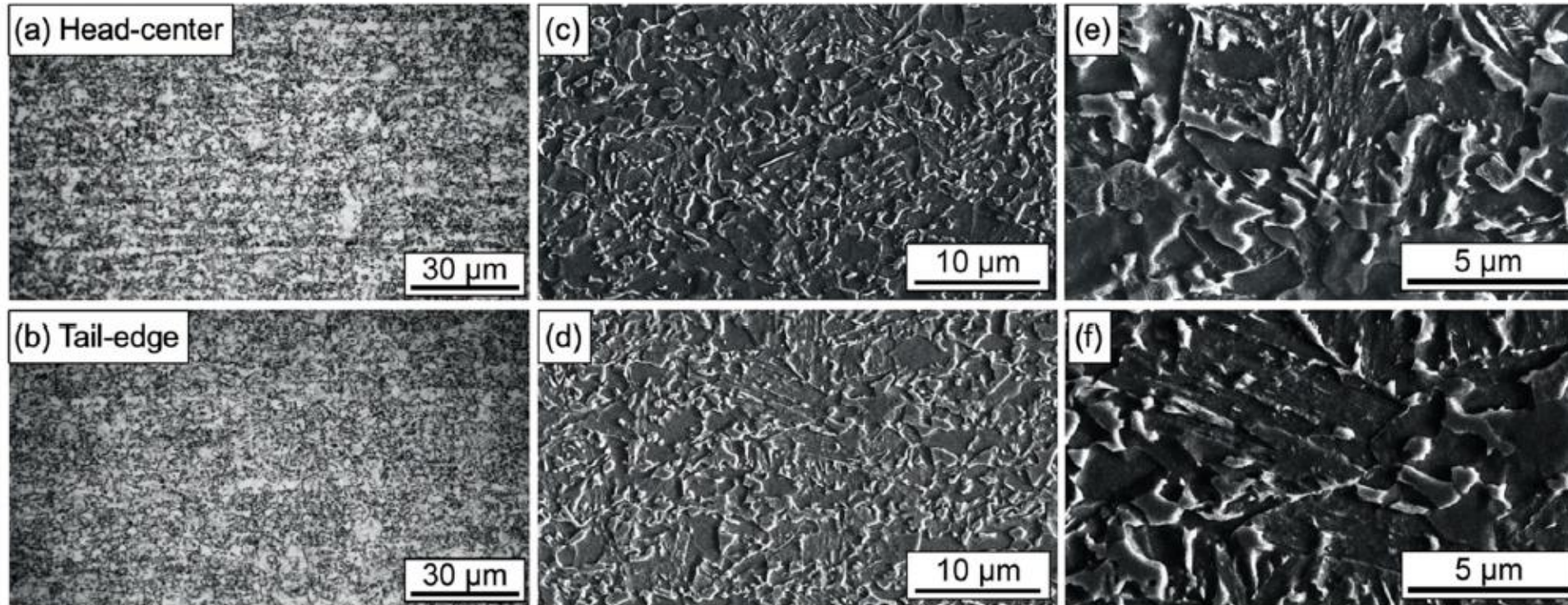
BATCH ANNEALED MICROSTRUCTURE



Microstructure of the subject steel in batch annealed condition: (a,b) light optical microscopy; (c,d) transmission electron microscopy.

Note retention of highly non-uniform structure in conjunction with spheroidization.

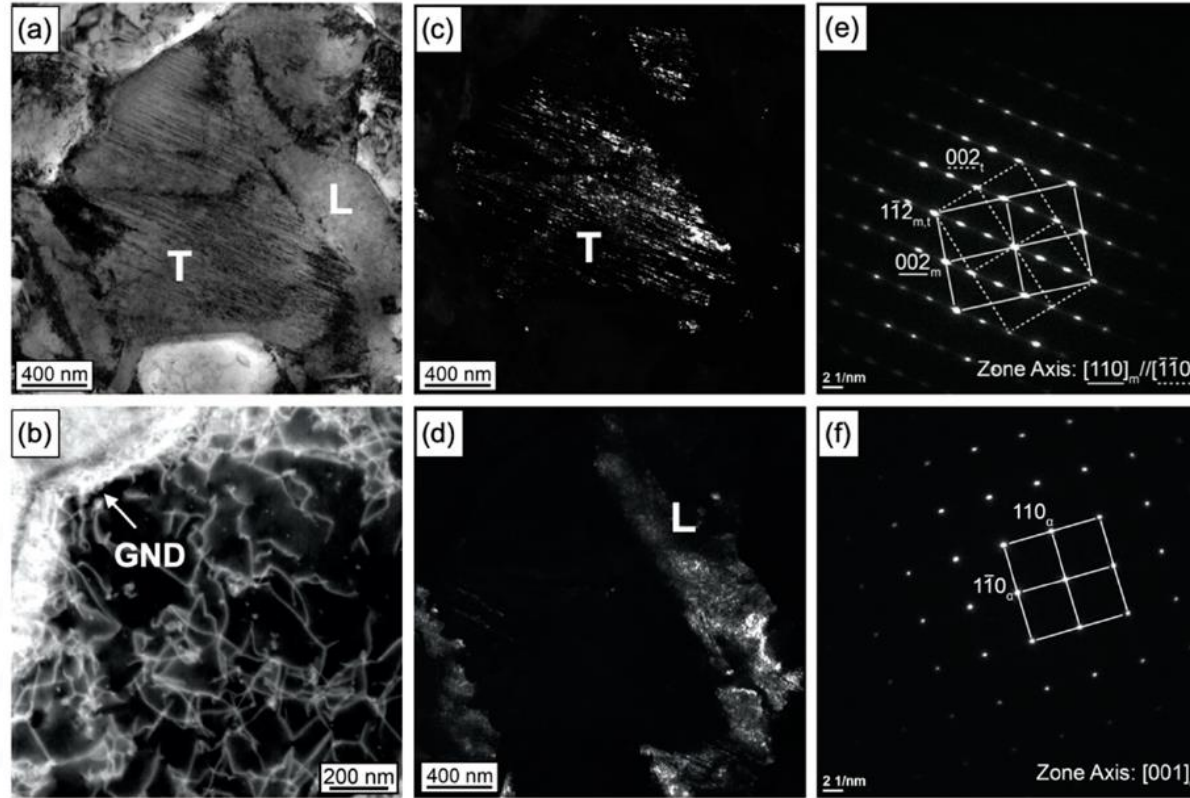
FINAL MICROSTRUCTURE



Microstructure of cold rolled steel after final continuous annealing: (a,b) light optical microscopy; (c-f) scanning electron microscopy.

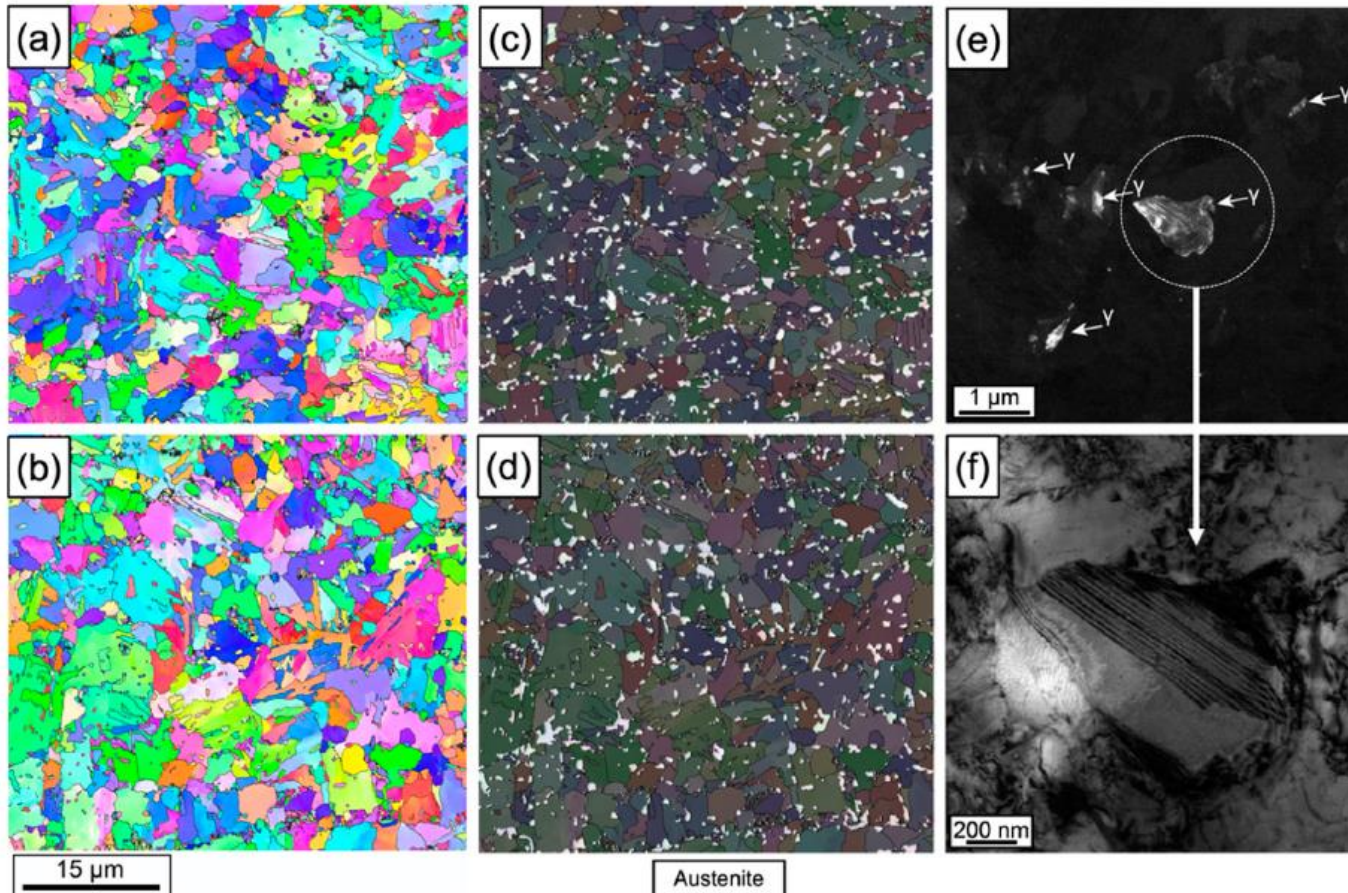
Homogeneity is recovered!

FINAL MICROSTRUCTURE



Identification of microstructural details after final conditioning by TEM: (a) coexistence of lath (L) and twinned (T) martensite; (b) geometrically necessary dislocations (GND) at boundary between ferrite and martensite; (c,e) twinned martensite; (d,f) lath martensite.

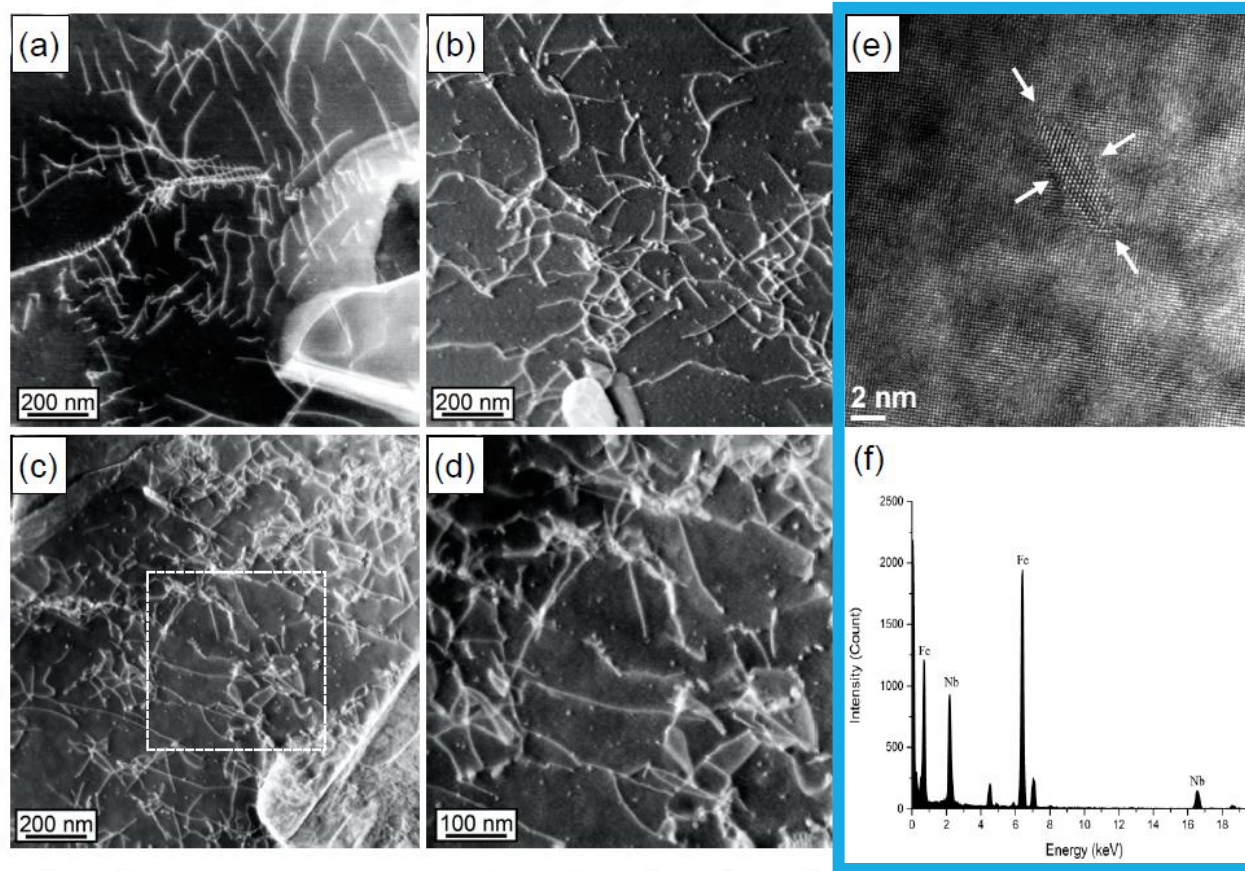
PHASE FRACTION EVALUATION



Position in Strip	Phase Share (%)		
	Ferrite	Martensite	Austenite
Head-center	44	48	8
Head-edge	46	46	8
Tail-center	45	48	7
Tail-edge	42	52	6

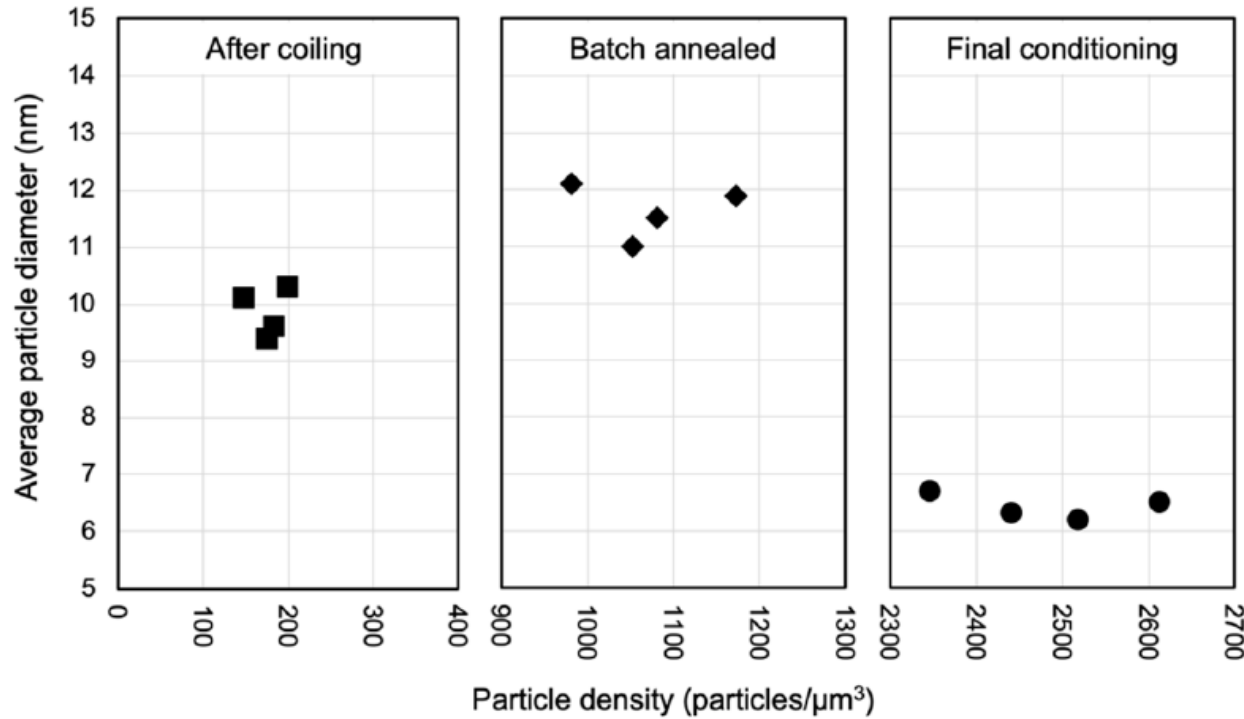
Characterization of final DP microstructure: (a,c) head-center, (b,d) tail-edge and identification of the retained austenite phase (white colored grains on the EBSD background (c,d)); TEM characterization of austenite grains: (e) dark field image, (f) bright field image of detail in (e).

NIوبيUM PRECIPITATE EVOLUTION



Evolution of niobium precipitation during processing stages characterized by TEM: (a) as hot rolled; (b) after batch annealing; (c) after hot dip galvanizing; (d) higher magnification of dashed area marked in (c); (e) representative high-resolution image of NbC precipitate in ferrite matrix after batch annealing; (f) EDX spectrum indicating a high level of Nb in the precipitates

NIOBIUM PRECIPITATE EVOLUTION

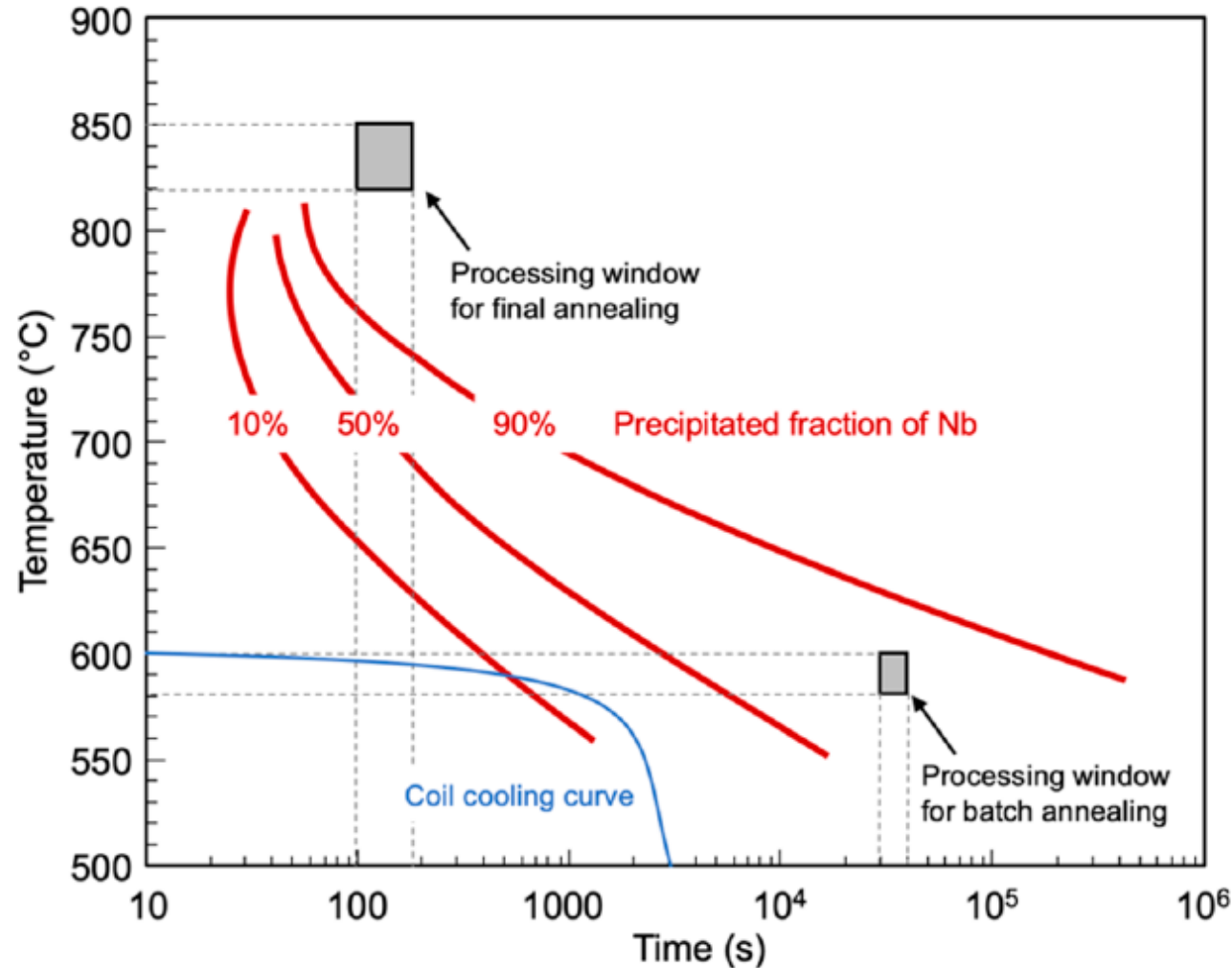


Size and particle density analysis of niobium precipitates for the different processing conditions at four strip positions.

Processing Stage	Particle Size (nm)	Particle Count (μm^{-3})	Particle Volume Fraction (%)	Amount (ppm)/Share (%) of Precipitated Nb
Hot rolled	9.6	188	0.004	35/10%
Batch annealed	11.6	1072	0.023	~200/~70% ¹
Final conditioning	6.5	2480	0.034	303/100%

¹ estimated value based on observed particle diameter-to-thickness ratio

NIOBIUM PRECIPITATE EVOLUTION & STRENGTH INCREMENT



Precipitation kinetics of niobium in the ferrite phase; various time-temperature scenarios applied during processing of DP steel in the current study are indicated. Final A-O calculation of NbC contribution to ferrite strength is ≈ 80 MPa.

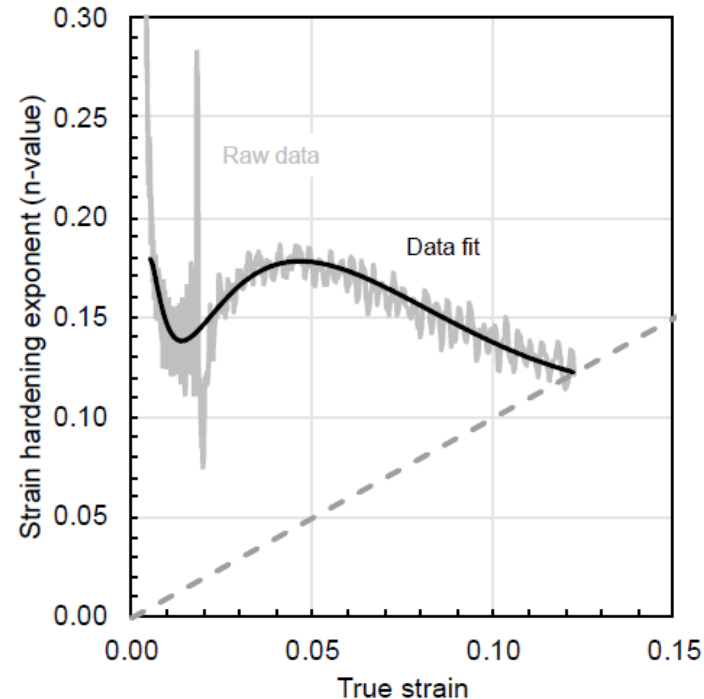
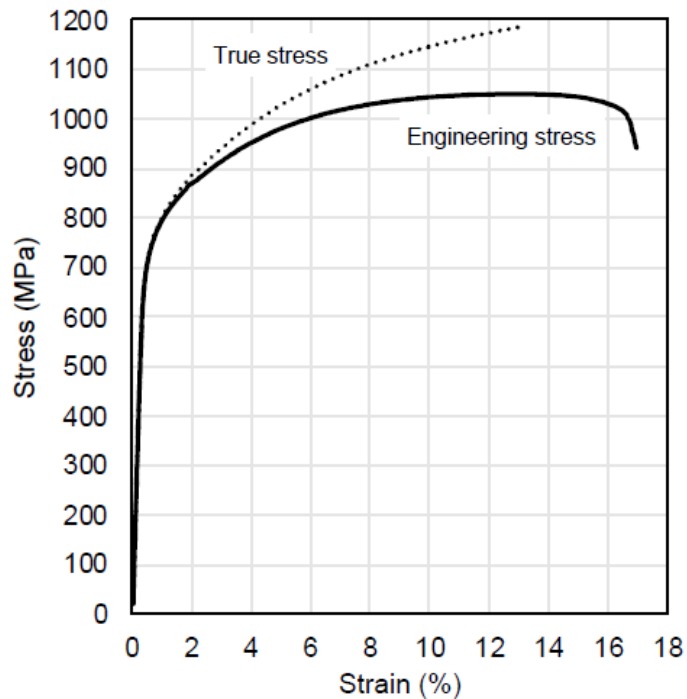
$$\sigma_{\text{Ashby-Orowan}} = \frac{0.8 \cdot M \cdot G \cdot b}{2\pi \cdot L \sqrt{1 - \nu}} \cdot \ln\left(\frac{x}{2b}\right)$$

MECHANISTIC DISCUSSION

- Batch annealing coarsens both NbC and cementite and alters recrystallization/austenitization sequence relative to standard processing.
 - Classic recrystallization kinetics asserts that iron carbide dissolution/coarsening is limiting process (Bunge et al.)
 - Austenite nucleation preferentially occurs at ferrite and cementite boundaries
- Concurrent austenitization / recrystallization results from a strong suppression of ferrite recrystallization and reduction of Ac temperatures due to C and Mn additions.
- High ferrite defect density drives high austenite nucleation density and carbides assist in pinning subsequent growth.
- Retained austenite distribution is dictated by distribution of former cementite particles, and batch annealing further assists in localization of C and Mn for austenite retention upon cooling.

MECHANICAL PROPERTIES

Steel Grade	Yield Strength $R_{p0.2}$ (MPa)	Tensile Strength R_m (MPa)	Elongation at Fracture A_{80} (%)	n-value	
				n_{4-6}	n_{10-20} / A_g
CR440Y780T-DH	440–550	780–900	≥18	≥0.18	≥0.13
CR700Y980T-DH	700–850	980–1180	≥13	-	-
Current production (typical values)	740	1030	15	≥0.14	≥0.12



CONCLUSIONS

CONCLUSIONS

- Niobium microalloying to dual phase steels significantly contributes to strength by both precipitation of ultrafine particles and microstructural refinement. A pronounced refinement of the DP microstructure is related to a strong recrystallization delay of the cold rolled ferrite matrix by NbC. The precipitates further restrict grain growth during the soaking phase of the final annealing cycle.
- In addition, properties relevant to formability are being improved due to known mechanisms of strain partitioning.
- Intermediate annealing results in both further fine NbC distributions and cementite spheroidization. Carbon and Mn localization as a result of the intermediate annealing is asserted as beneficial for subsequent austenite retention.

FOR MORE INFORMATION

Matt Enloe

CBMM North America

Matthew.Enloe@cbmm.com